nature communications

Article

https://doi.org/10.1038/s41467-025-60459-0

Consecutive mechanical-force-induced electron transfer for reduction of aryl halides with high reduction potentials

Received: 17 January 2025

Accepted: 22 May 2025

Published online: 04 June 2025

Check for updates

Xiaohong Wang[1,2], Xiaochun He[1,2], Xuemei Zhang[1,2], Qingqing Wang[1], Qian Huang[1], Ruiling Qu[1] & Zhong Lian[1]

Mechanical-force-induced redox catalysis has emerged as a green and expeditous approach in synthetic chemistry, relying on single-electron transfer from polarized piezoelectric materials to substrates initiated by mechanical agitation. However, the piezoelectric potential generated can sometimes be insufficient to activate the electron transfer process, similar to the limitations observed in photocatalytic reactions. In this work, we introduce a catalytic strategy employing a consecutive mechanical-force-induced electron transfer (ConMET) strategy. This strategy uses piezoelectric materials as mechanochemical redox catalysts with 9-phenyl-dihydroacridine as a sacrificial electron donor, enabling efficient consecutive electron transfer. Our method effectively reduces aryl iodides, bromides, and even electron-rich aryl chlorides, which possess reduction potentials as high as −2.8 V (vs. SCE), leading to the formation of aryl radicals. Ultimately, this strategy facilitates *anti*-Markovnikov hydroarylation of alkenes and dehalogenative deuteration of aromatic halides under mild conditions.

The pursuit of sustainable and environmentally friendly techniques for organic synthesis remains a significant challenge for organic chemists. Over the past decade, photocatalysis has rapidly advanced, providing numerous alternative solutions for synthetic chemistry[1–3]. To enhance light utilization efficiency, many studies have focused on the development of visible-light-driven photocatalysts. Effective harnessing of visible light, characterized by lower photon energy compared to ultraviolet light, has led to the establishment of various strategies, including consecutive photoinduced electron transfer (ConPET)[4–6], sensitization-initiated electron transfer (SenI-ET)[7–10], and electrophotocatalysis[11–16](Fig. 1a).

On the other hand, the emerging field of mechanoredox chemistry presents green, straightforward, and unconventional strategies for modern synthetic chemistry[17–23]. These approaches utilize mechanical agitation to polarize piezoelectric materials, facilitating the reduction of substrates into free radicals through a single-electron transfer (SET) process, thus enabling diverse chemical transformations[24–40]. This reduction results in the formation of a "hole", which is then returned to the unpolarized ground state through the single-electron oxidation of the appropriate electron donor, such as tris(2-pyridylmethyl)amine (TPMA)[41,42]. The intrinsic properties of these piezoelectric materials largely influence their capacity to initiate different types of reactions[43]. In certain circumstances, however, the generated piezoelectric potential may not suffice to initiate the reduction process, analogous to the limitations of visible-light excitation in photocatalytic reactions. This issue has sparked our interest in developing effective solutions.

Aryl radicals are highly adaptable synthetic intermediates in organic chemistry and also demonstrate intriguing biological functions, particularly in mechanisms such as DNA cleavage[44]. Aryl radicals are typically generated through the reduction of aryl diazonium[45,46], iodonium[47,48], and sulfonium salts[49], or *via* the oxidation of benzoates[50]. However, the preparation of these

[1]Department of Dermatology, State Key Laboratory of Biotherapy and Cancer Center, West China Hospital, Sichuan University, Chengdu 610041, China. [2]These authors contributed equally: Xiaohong Wang, Xiaochun He, Xuemei Zhang. e-mail: lianzhong@scu.edu.cn

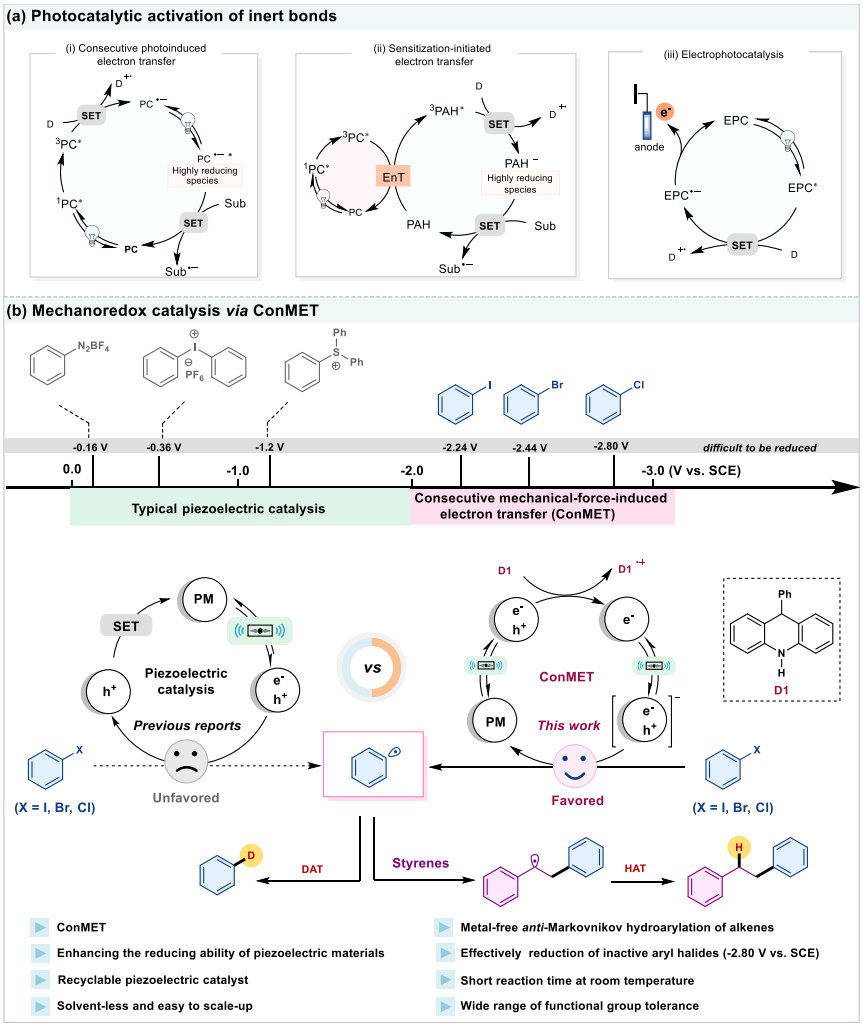

Fig. 1 | Development of inert bond activation *via* photoredox catalysis and mechanoredox catalysis. a Photocatalytic activation of inert bonds. **b** This work: Mechanoredox catalysis *via* ConMET.

precursors can often be difficult due to stability issues or the necessity for harsh reaction conditions, which has somewhat restricted their use, particularly in large-scale applications[51]. In comparison, aryl halides present distinct advantages in terms of stability and accessibility, which simplifies handling and storage, thereby enhancing their practicality and efficiency for various synthetic applications[52–56]. Nevertheless, aryl halides possess significantly higher reduction potentials (E_{red} ≈ −2.24 V ~ −2.80 V vs. SCE) than aryl diazonium (E_{red} ≈ −0.16 V vs. SCE) and diaryliodonium salts (E_{red} ≈ −0.36 V vs. SCE). This difference is primarily attributable to the higher activation energy barriers associated with the cleavage of the C(sp^2)–X bond, which presents considerable challenges for converting aryl halides into aryl radicals[57,58]. To date, there are few documented instances of employing piezoelectric catalytic processes to facilitate this type of transformation[59]. Enlightened by the consecutive photoinduced electron transfer (ConPET) strategy in photoredox catalysis[4–6], which overcomes the energetic limitation of visible light by utilizing two photons and an additional electron donor to generate highly reducing species within a single catalytic cycle, our research team aims to develop an unusual approach within the realm of mechanoredox chemistry. We propose the consecutive mechanical-force-induced electron transfer (ConMET) strategy to address the challenges associated with the strong reduction capability required for the reduction of aryl halides (Fig. 1b). This method utilizes a sacrificial electron donor (**D1**) that transfers an electron to the polarized piezoelectric material upon mechanical milling. Continued mechanical agitation further excites this piezoelectric material, enhancing its reducing capacity. Therefore, the key to implementing this strategy hinges on the selection of appropriate piezoelectric materials and sacrificial electron donors to ensure that the generated reducing species possess sufficient reducing ability to convert aryl halides into aryl radicals, which present high activation energy barriers.

In this study, we demonstrate that the combination of piezoelectric materials and 9-phenyldihydroacridine (**D1**) can effectively support a ConMET process, establishing a piezoelectric catalytic system containing strong reducing species within the context of mechanochemistry.

This system efficiently reduces unactivated and even electron-rich aryl halides with reduction potentials as high as −2.80 V (vs. SCE), facilitating the formation of aryl radicals. These aryl radicals can participate in various reactions, including *anti*-Markovnikov hydroarylation of alkenes and dehalogenative deuteration of aromatic halides. This strategy offers several advantages, such as the elimination of transition metals, operational simplicity, and mild reaction conditions. It has also proven effective for complex pharmaceutical molecules during late-stage derivatizations.

https://doi.org/10.1038/s41467-025-60459-0

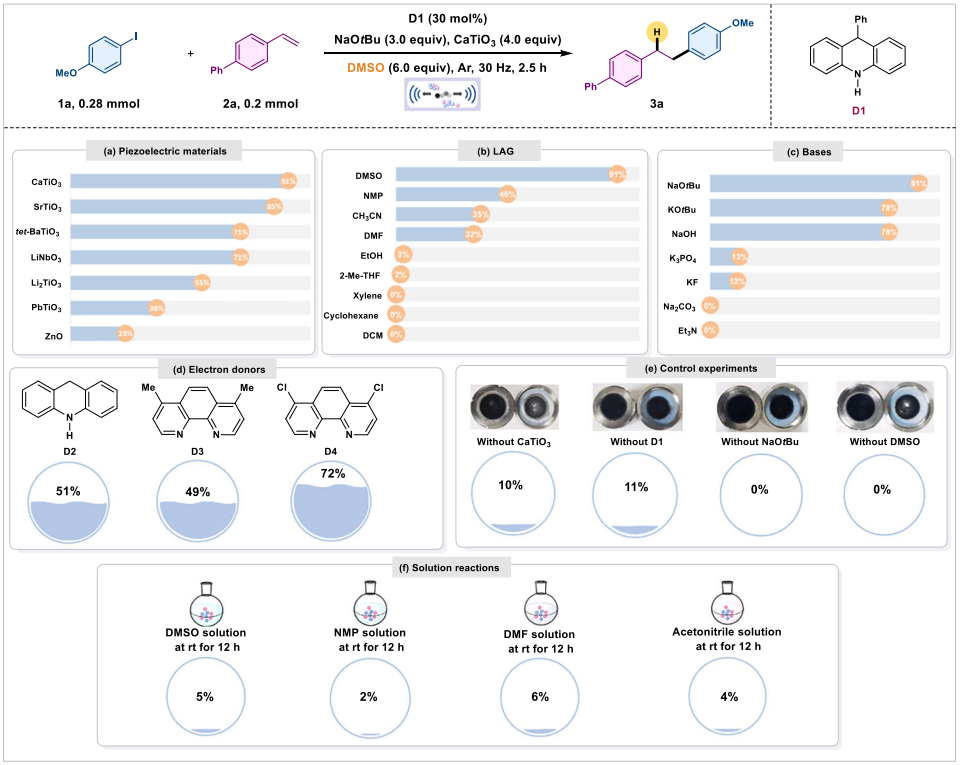

Fig. 2 | The optimization of reaction conditions. Reaction Conditions: **1a** (0.28 mmol, 1.4 equiv), **2a** (0.20 mmol, 1.0 equiv), **D1** (0.06 mmol, 30 mol%), NaO*t*Bu (0.6 mmol, 3.0 equiv), $CaTiO_3$ (0.8 mmol, 4.0 equiv), DMSO (1.2 mmol, 6.0 equiv) in a stainless-steel jar (10 mL) with two balls (10 mm) in Ar; ball milling conditions: 2.5 h at 30 Hz; yields were determined by GC using dodecane as an internal standard. **a** The optimization of piezoelectric materials; **b** The optimization of liquid assisted grinding (LAG); **c** The optimization of bases; **d** The optimization of electron donors; **e** Control experiments; **f** Solution reactions, rt: room temperature.

Results

Reaction optimization

In the initial phase of our study, we explored the feasibility of implementing hydroarylation of alkenes using aryl halides under mechanochemical conditions. We employed 4-methoxyiodobenzene (**1a**) and 4-vinylbiphenyl (**2a**) as model substrates, with 9-phenyldihydroacridine (**D1**) serving as the sacrificial electron donor. DMSO was utilized both as a hydrogen source and as a liquid assisted grinding (LAG) agent, while NaO*t*Bu was used as the base, together with a piezoelectric material to facilitate the reaction under ball-milling conditions (Fig. 2). Notably, various piezoelectric materials proved effective for this transformation, successfully yielding the target product **3a** and thereby supporting the rationale for our proposed pathway. Among the tested piezoelectric materials, $CaTiO_3$ exhibited the best performance, achieving a remarkable yield of 91% for product **3a** (Fig. 2a). Substituting DMSO with alternative solvents resulted in reduced product yields. When polar aprotic solvents, such as *N*-methyl-2-pyrrolidone (NMP), acetonitrile, and dimethylformamide (DMF) were tested as substitutes, product **3a** was obtained in yields ranging from 32% to 46%. While the use of polar protic solvents like ethanol, as well as ethers and non-polar aprotic solvents including toluene, cycloalkane, and dichloromethane (DCM), nearly completely inhibited the hydroarylation process (Fig. 2b). A screening of various bases showed that NaO*t*Bu outperformed all other bases in terms of reaction efficiency (Fig. 2c).

Additionally, we replaced the sacrificial electron donor **D1** with other molecules of analogous skeleton, such as 9, 10-hydroacridine (**D2**), substituted *O*-phenanthrolines (**D3**-**D4**) and other electron donors (**D5**-**D10**) (Fig. 2d and Table S1). However, these alternatives led to inferior transformation efficiencies compared to **D1**.

Subsequently, we conducted a series of controlled experiments to assess the necessity of each reaction component (Fig. 2e). The results revealed that the exclusion of either the sacrificial electron donor **D1** or the piezoelectric material $CaTiO_3$ resulted in a substantial reduction in the yield of **3a**. Furthermore, the elimination of NaO*t*Bu or DMSO completely inhibited the reaction, underscoring the essential role of all these components in facilitating the transformation. Additionally, reactions were conducted in various solvents within a glass setup at room temperature. Stirring the reactants in DMSO, NMP, DMF, and CH_3CN for 12 h produced only a trace amount of the anticipated product **3a**, and these results highlight the crucial function of mechanical force in the hydroarylation process. (Fig. 2f).

Substrate scopes

We next investigate the substrate scope of the hydroarylation of alkene under the optimized reaction conditions (Fig. 3). First, a diverse range of mono- and poly-substituted aryl iodides were evaluated in this transformation. Aryl iodides containing various electron-donating substituents (-OMe, $-OCH_2Ph$, -OAr, -Ph, -Me, -*t*Bu, $-NR_2$) at different positions on the benzene ring were found to be compatible with the reaction conditions, yielding products (**3a**-**3i**) in moderate to high yields. Additionally, aryl iodides featuring strong electron-withdrawing groups, including $-OCF_3$ (**3j, 3k**) and $-CF_3$ (**3l**), were tolerated in the transformation. Notably, when *para*-fluoro or *para*-chloro substituted aryl iodides were utilized, the reaction selectively cleaved the more reactive C–I bond rather than the C–F or C–Cl bonds (**3m, 3n**). Furthermore, polycyclic aryl iodides, including 9-iodophenanthrene (**3o**) and fluoranthene (**3p**), proved suitable for this reaction. Heteroaryl iodides derived from pyridine (**3q**), thiophene (**3r**), and pyrazole (**3s**), were also successfully incorporated into the reaction, yielding target products with moderate efficiency. Subsequently, the scope of aryl alkenes was explored in the reaction. Both *p*-methyl-substituted styrene and 2-vinylnaphthalene were found to produce the desired

https://doi.org/10.1038/s41467-025-60459-0

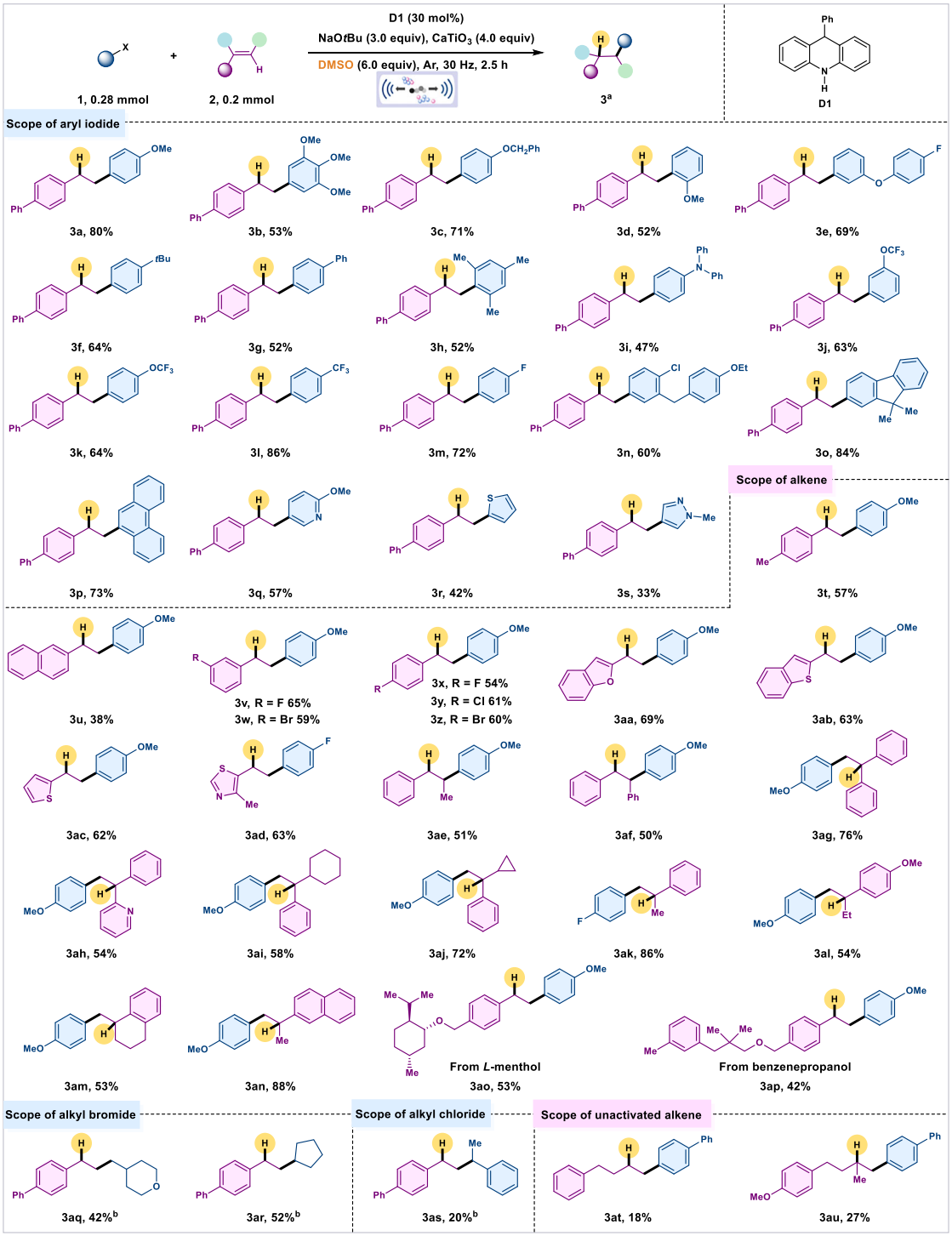

Fig. 3 | Substrate scope of *anti*-Markovnikov hydroarylation of alkenes. a **1** (0.28 mmol, 1.4 equiv), **2** (0.20 mmol, 1.0 equiv), **D1** (0.06 mmol, 30 mol%), NaO*t*Bu (0.6 mmol, 3.0 equiv), $CaTiO_3$ (0.8 mmol, 4.0 equiv), DMSO (1.2 mmol, 6.0 equiv) in a stainless-steel jar (10 mL) with two balls (10 mm) in Ar; ball milling conditions: 2.5 h at 30 Hz, isolated yields. **b** 0.6 mmol alkyl bromides or alkyl chloride.

products (**3t, 3u**) in medium yields. Halogen-substitutions on the phenyl ring of styrene also proved viable in this context (**3v**-**3z**). Notably, heterocyclic substrates containing benzofuran (**3aa**), benzothiophene (**3ab**), thiophene (**3ac**), and thiazole (**3ad**) moieties could also smoothly go through the transformation.

Further investigation revealed that the reactivity of internal olefins was largely unaffected when substituting the *β*-methyl group (**3ae**) with a bulky phenyl group (**3af**). A wide range of internal styrenes, including those containing phenyl (**3ag**), pyridyl (**3ah**), cycloalkyl (**3ai, 3aj**), and alkyl (**3ak, 3al**) were also tolerated, providing corresponding products in moderate to excellent yields. Cyclic alkene (**3am**) and *α*-methyl-substituted 2-naphthoethylene (**3an**) were also amenable to the reaction, generating hydroarylated products with yields of 53% and 88%, respectively. To illustrate the broad applicability of this

https://doi.org/10.1038/s41467-025-60459-0

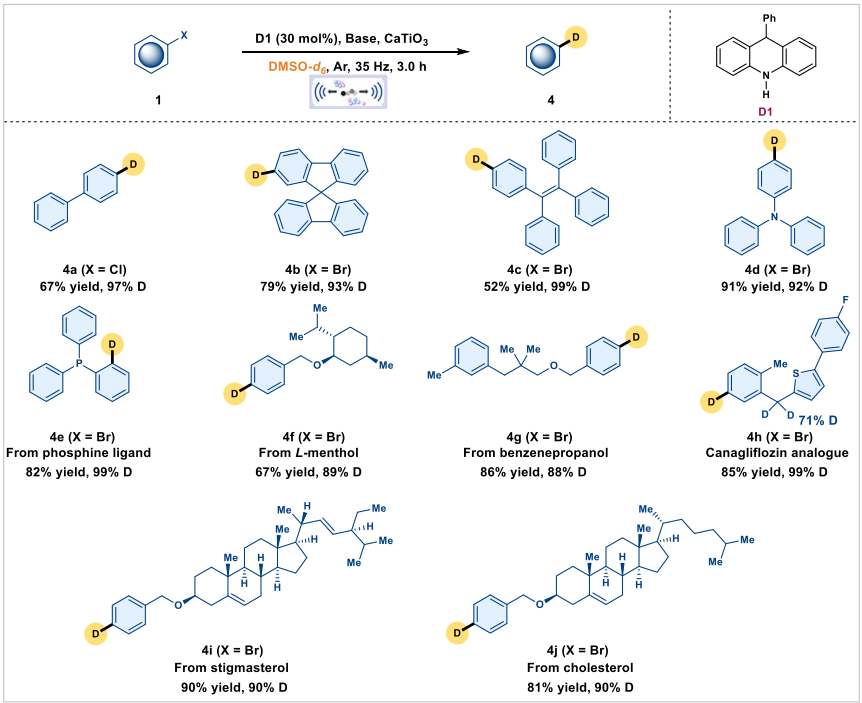

Fig. 4 | Substrate scope of mechanochemically driven dehalogenative deuteration. Aryl bromides (0.2 mmol, 1.0 equiv), **D1** (0.06 mmol, 30 mol%), KOH (0.28 mmol, 1.4 equiv or 0.6 mmol for **4i** and **4j**), $CaTiO_3$ (0.8 mmol, 4.0 equiv) and DMSO-d_6 (0.4 mmol, 2.0 equiv or 1.2 mmol for **4i** and **4j**) in a stainless-steel jar (10 mL) with two balls (10 mm) in Ar; ball milling conditions: 3.0 h at 35 Hz, isolated yields. Aryl chlorides (0.4 mmol, 1.0 equiv), **D1** (0.12 mmol, 30 mol%), KO*t*Bu (0.56 mmol, 1.4 equiv), $CaTiO_3$ (1.6 mmol, 4.0 equiv), and DMSO-d_6 (2.4 mmol, 6.0 equiv) in a stainless-steel jar (10 mL) with two balls (10 mm) in Ar; ball milling conditions: 3.0 h at 35 Hz, isolated yields.

methodology, we applied it to the late-stage functionalization of pharmacologically active molecules. Pharmaceutical compounds derived from styrenes, such as *L*-menthol (**3ao**) and benzenepropanol (**3ap**), were successfully converted into their corresponding hydroarylation products. We subsequently examined the reactivity of alkyl bromides and alkyl chlorides. The results indicated that both primary and secondary alkyl bromides can efficiently produce *anti*-Markovnikov hydroarylation products from the corresponding alkenes, yielding moderate results (**3aq, 3ar**). In contrast, when alkyl chloride was used as a substrate, the yield of the desired product was severely restricted, achieving only 20% (**3as**). Finally, we investigated the reactivity of unactivated alkenes in the mechanochemical *anti*-Markovnikov hydroarylation of alkenes. The results indicated that only approximately 20% of the target products were obtained (**3at, 3au**).

In the following study, we investigated the dehalogenative deuteration of aryl halides using the ConMET strategy under ball milling conditions (Fig. 4). Pleasingly, aryl chloride underwent the deuteration smoothly, offering the desired product **4a** with a 67% yield and 97% deuterium incorporation. Additionally, a bromide substrate containing polycyclic aromatic rings produced the corresponding product **4b** in a high yield, accompanied by a remarkable deuterium incorporation rate. Substrates with alkene (**4c**), amine (**4d**) functionalities were also tolerated in the reaction conditions. Interestingly, a bromine-containing phosphine ligand (**4e**) successfully underwent the transformation with a high yield and a significant deuterium incorporation rate. Furthermore, we applied this dehalogenative deuteration method in deuterium labeling of various complex derivatives of bioactive molecules and pharmaceuticals (**4f**–**4j**), all of which achieved commendable yields and exceptional deuterium incorporation rates.

To demonstrate the scalability and effectiveness of hydroarylation of alkenes *via* a mechanochemical process, we conducted the transformation of compound **2a** on a 2.5 mmol scale, producing the desired product **3a** with an impressive 83% yield (Fig. 5a). In addition, we performed recycling experiments with $CaTiO_3$ to assess the catalytic efficiency of the recycled piezoelectric material (Fig. 5b). After each reaction producing **3a**, $CaTiO_3$ was filtered and washed for reuse in the subsequent cycle. The yield of product **3a** remained consistent during the first three cycles but declined to 58% starting from the fourth cycle. This decrease is likely due to a progressive reduction in the particle size of $CaTiO_3$, which adversely affected its piezoelectric properties[60–63]. The particle size of piezoelectric materials can be enhanced through sintering and standard solid-state processing methods[62,64], enabling the recycling of these materials.

Mechanistic investigations

In order to elucidate the detailed mechanism of hydroarylation of alkenes with alkyl halides, we conducted several experiments. Under standard conditions except for replacing DMSO with DMSO-d_6, a deuterated hydroarylation product **D-3a** was obtained with a good yield and 99% deuterium incorporation (Fig. 5c). This result indicates that DMSO, rather than **D1**, serves as the hydrogen atom donor (HAD) in this hydroarylation process. The addition of radical scavengers, namely 2,2,6,6-tetramethyl-1-piperinedinyloxy (TEMPO) and butylated hydroxytoluene (BHT), nearly completely inhibited the reactions. Aryl radical adduct **5** and benzyl radical adduct **6** were detected by high-resolution mass spectrometry (HRMS) upon the addition of TEMPO (Fig. 5c), suggesting the involvement of a radical pathway. Utilizing this mechanochemical strategy, the reaction between reactant **1a** and cyclopropane-containing alkene **7** afforded the ring-opening product **9** (Fig. 5d), which provides compelling evidence for the involvement of alkyl radical intermediate **8** in the transformation. These results imply that aryl radicals are likely generated during the process.

This study investigated the crystal structure of $CaTiO_3$ nanoparticles using high-resolution X-ray diffraction (XRD). The findings indicate that the crystal structure of $CaTiO_3$ nanoparticles remained

https://doi.org/10.1038/s41467-025-60459-0

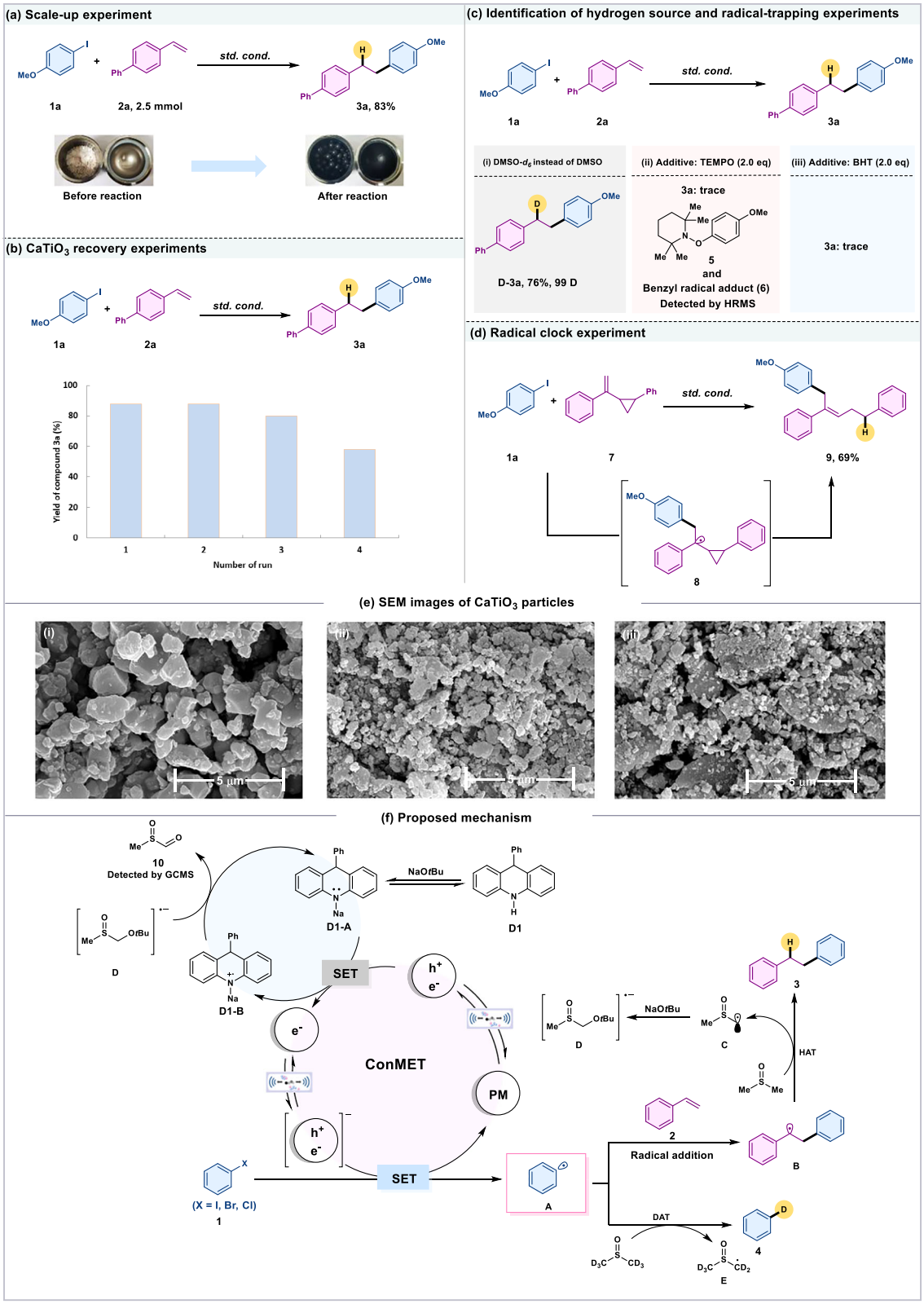

Fig. 5 | Study of reaction applications and mechanisms. a Scale-up experiment. **b** $CaTiO_3$ recovery experiments. **c** Identification of hydrogen source and radical-trapping experiments. **d** Radical clock experiment. **e** SEM images of $CaTiO_3$ particles (i) before reaction; (ii) after reaction; (iii) after 4 cycles. **f** Proposed mechanism.

unchanged before and after grinding (Fig. S9). Additionally, we analyzed the morphology and size of $CaTiO_3$ particles before and after the reaction using scanning electron microscopy (SEM). This analysis revealed substantial mechanical deformation and alterations in particle size under mechanical stress (Fig. 5e). The commercial $CaTiO_3$ particles exhibited an average particle size of approximately 1 μm (Fig. 5e (i)). However, following ball milling at 30 Hz for 2.5 h during the first reaction round, notable morphological changes and size variations were observed (Fig. 5e (ii)). After four cycles of reuse, the size of the $CaTiO_3$ particles decreased significantly, presenting an irregular

size range of approximately 90 nm to 900 nm, along with agglomerations (Fig. 5e (iii)). These agglomerations may contribute to the reduced yield of the target product in the aforementioned piezoelectric material recycling experiments[65,66] (Fig. 5b).

Proposed mechanism

Based on our findings, we propose a plausible mechanism for the hydroarylation of alkenes and the dehalogenative deuteration of aryl halides *via* consecutive mechanical-force-induced electron transfer (ConMET) pathway (Fig. 5f). The interaction between 9-phenyldihydroacridine (**D1**) and NaO*t*Bu produces intermediate **D1-A**. Meanwhile, mechanical agitation induces polarization in $CaTiO_3$ particles. These highly polarized $CaTiO_3$ particles then undergo a single-electron reduction facilitated by intermediate **D1-A**. This process produces a radical cationic species (**D1-B**) and reduced $CaTiO_3$ particles. Further mechanical-force stimulation energizes the reduced $CaTiO_3$ particles, providing more powerful reducing species called super electron donors. These super electron donors then participate in a single-electron transfer (SET) process with aryl halides, resulting in the formation of reactive aryl radicals (**A**) and the regeneration of the ground-state $CaTiO_3$. Subsequently, the aryl radical (**A**) adds to an alkene in an *anti*-Markovnikov fashion, leading to the formation of an alkyl radical intermediate (**B**), which would obtain a hydrogen from DMSO *via* a hydrogen atom transfer (HAT) process. This reaction concurrently yields the hydroarylation product (**3**) and a carbon radical species (**C**). Radical **C** then reacts with NaO*t*Bu to form the radical anion species (**D**), which facilitates the closure of the electron donor (**D1**) catalyst cycle and ultimately produces the corresponding by-product (**10**). On the other hand, the aryl radical (**A**) reacts with DMSO-d_6 through a deuterium atom transfer (DAT) pathway, resulting in the formation of the dehalogenative deuteration product **4** (for the dehalogenative deuteration process).

In conclusion, we have developed a piezoelectric catalytic system functioning through a ConMET pathway. This system utilizes a piezoelectric material $CaTiO_3$, and a sacrificial electron donor, 9-phenyldihydroacridine **D1**, to enable the generation of catalytic species with exceptionally high reducing power, thereby facilitating the reduction of aryl halides (Cl, Br, I) with high reduction potentials to aryl radicals. Employing this system enables a range of reactions, including *anti*-Markovnikov hydroarylation of alkenes and dehalogenative deuteration of aromatic halides. This system has several advantages, such as low cost, absence of metal catalysts, and mild operation conditions, which allow for wide applications within the synthetic community. This work showcases a ConMET mechanism in mechanoredox chemistry, providing a valuable reference for the design of other mechanochemical catalytic reactions.

Methods

anti-Markovnikov hydroarylation of alkenes

Aryl iodides (**1**, 0.28 mmol, 1.4 equiv) or alkyl bromides or alkyl chloride (**1**, 0.6 mmol, 3.0 equiv), alkenes (**2**, 0.20 mmol, 1.0 equiv), promoter (**D1**, 0.06 mmol, 30 mol%), NaO*t*Bu (0.6 mmol, 3.0 equiv), and $CaTiO_3$ (0.8 mmol, 4.0 equiv) were placed in a stainless-steel milling jar (10.0 mL) with two stainless-steel balls (10 mm, diameter) in air. DMSO (1.2 mmol, 6.0 equiv) was added into the jar in the argon-filled glovebox, the jar was placed in powteq vibration ball mill GT300 (30 Hz). After grinding for 2.5 h (30 min break 5 min for five times), the reaction mixture was washed with ethyl acetate. The solvent was evaporated in vacuo, and the remaining residue was purified by column chromatography on silica gel to yield products.

Dehalogenative deuteration of aromatic bromides and aromatic chlorides

Aryl bromides (0.2 mmol, 1.0 equiv), promoter (**D1**, 0.06 mmol, 30 mol %), KOH (0.28 mmol, 1.4 equiv or 0.6 mmol for **4i** and **4j**) and $CaTiO_3$ (0.8 mmol, 4.0 equiv) were placed in a stainless-steel milling jar (10.0 mL) with two stainless-steel balls (10 mm, diameter) in air. DMSO-d_6 (0.4 mmol, 2.0 equiv or 1.2 mmol for **4i** and **4j**) was added into the jar in the argon-filled glovebox, the jar was placed in powteq vibration ball mill GT600 (35 Hz). After grinding for 3.0 h (10 min break 5 min for eighteen times), the reaction mixture was washed with ethyl acetate. The solvent was evaporated in vacuo, and the remaining residue was purified by column chromatography on silica gel to yield products. Aryl chlorides (0.4 mmol, 1.0 equiv), promoter (**D1**, 0.12 mmol, 30 mol %), KO*t*Bu (0.56 mmol, 1.4 equiv), and $CaTiO_3$ (1.6 mmol, 4.0 equiv) were placed in a stainless-steel milling jar (10.0 mL) with two stainless-steel balls (10 mm, diameter) in air. DMSO-d_6 (2.4 mmol, 6.0 equiv) was added into the jar in the argon-filled glovebox, the jar was placed in powteq vibration ball mill GT600 (35 Hz). After grinding for 3.0 h (10 min break 5 min for 18 times), the reaction mixture was washed with ethyl acetate. The solvent was evaporated in vacuo, and the remaining residue was purified by column chromatography on silica gel to yield products.

Data availability

All data from this study are provided in the published article and its Supplementary Information file. Detailed experimental procedures, NMR, and HRMS analysis data can be found in the Supplementary Information. For further inquiries, data can be obtained by contacting the corresponding author.

References

1. Bauer, A., Westkämper, F., Grimme, S. & Bach, T. Catalytic enantioselective reactions driven by photoinduced electron transfer. *Nature* **436**, 1139–1140 (2005).
2. Nicewicz, D. A. & MacMillan, D. W. C. Merging photoredox catalysis with organocatalysis: the direct asymmetric alkylation of aldehydes. *Science* **322**, 77–80 (2008).
3. Prier, C. K., Rankic, D. A. & MacMillan, D. W. C. Visible light photoredox catalysis with transition metal complexes: applications in organic synthesis. *Chem. Rev.* **113**, 5322–5363 (2013).
4. Glaser, F., Kerzig, C. & Wenger, O. S. Multi-photon excitation in photoredox catalysis: concepts, applications, methods. *Angew. Chem. Int. Ed.* **59**, 10266–10284 (2020).
5. Goez, M., Kerzig, C. & Naumann, R. An "all-green" catalytic cycle of aqueous photoionization. *Angew. Chem. Int. Ed.* **53**, 9914–9916 (2014).
6. Cybularczyk-Cecotka, M., Szczepanik, J. & Giedyk, M. Photocatalytic strategies for the activation of organic chlorides. *Nat. Catal.* **3**, 872–886 (2020).
7. Ghosh, I., Shaikh, R. S. & König, B. Sensitization-initiated electron transfer for photoredox catalysis. *Angew. Chem. Int. Ed.* **56**, 8544–8549 (2017).
8. Pal, A. K., Li, C. F., Hanan, G. S. & Zysman-Colman, E. Blue-emissive cobalt (III) complexes and their use in the photocatalytic trifluoromethylation of polycyclic aromatic hydrocarbons. *Angew. Chem. Int. Ed.* **57**, 8027–8031 (2018).
9. Coles, M. S., Quach, G., Beves, J. E. & Moore, E. G. A photophysical study of sensitization-initiated electron transfer: insights into the mechanism of photoredox activity. *Angew. Chem. Int. Ed.* **59**, 9522–9526 (2020).
10. Sun, X. et al. Asymmetric photoredox catalytic formal de Mayo reaction enabled by sensitization-initiated electron transfer. *Nat. Chem.* **16**, 1169–1176 (2024).
11. Lamb, M. C. et al. Electrophotocatalysis for organic synthesis. *Chem. Rev.* **124**, 12264–12304 (2024).
12. Barham, J. P. & König, B. Synthetic photoelectrochemistry. *Angew. Chem. Int. Ed.* **59**, 11732–11747 (2020).
13. Wu, S., Kaur, J., Karl, T. A., Tian, X. & Barham, J. P. Synthetic molecular photoelectrochemistry: new frontiers in synthetic

applications, mechanistic insights and scalability. *Angew. Chem. Int. Ed.* **61**, e202107811 (2022).
14. Huang, H., Steiniger, K. A. & Lambert, T. H. Electrophotocatalysis: combining light and electricity to catalyze reactions. *J. Am. Chem. Soc.* **144**, 12567–12583 (2022).
15. Chen, Y. J. et al. Transition-metal-free, site-selective C–F arylation of polyfluoroarenes *via* electrophotocatalysis. *J. Am. Chem. Soc.* **144**, 17261–17268 (2022).
16. Kim, H., Kim, H. J., Lambert, T. H. & Lin, S. Reductive electrophotocatalysis: merging electricity and light to achieve extreme reduction potentials. *J. Am. Chem. Soc.* **142**, 2087–2092 (2020).
17. Liu, R. X. et al. Organic reactions enabled by mechanical force-induced single electron transfer. *Chem. Eur. J.* **30**, e202401376 (2024).
18. Leitch, J. A. & Browne, D. L. Mechanoredox chemistry as an emerging strategy in synthesis. *Chem. Eur. J.* **27**, 9721–9726 (2021).
19. Ren, Z. Y. et al. Piezoelectrically mediated reactions: from catalytic reactions to organic transformations. *Chin. J. Chem.* **41**, 111–128 (2023).
20. Xia, H. S. & Wang, Z. H. Piezoelectricity drives organic synthesis. *Science* **366**, 1451–1452 (2019).
21. Ayarza, J., Wang, Z., Wang, J., Huang, C. W. & Esser-Kahn, A. P. 100th Anniversary of macromolecular science viewpoint: piezoelectrically mediated mechanochemical reactions for adaptive materials. *ACS Macro Lett.* **9**, 1237–1248 (2020).
22. Jiang, S. & Wang, M. A review on piezoelectric-mediated mechanoredox reactions by ball milling in organic synthesis. *Curr. Org. Chem.* **28**, 905–913 (2024).
23. Sheikhaleslami, S. & Sperry, J. Mechanochemical radical transformations in organic synthesis. *Chem. Eur. J.* **31**, e202403833 (2024).
24. Kubota, K., Pang, Y., Miura, A. & Ito, H. Redox reactions of small organic molecules using ball milling and piezoelectric materials. *Science* **366**, 1500–1504 (2019).
25. Schumacher, C., Hernández, J. G. & Bolm, C. Electromechanochemical atom transfer radical cyclizations using piezoelectric $BaTiO_3$. *Angew. Chem. Int. Ed.* **59**, 16357–16360 (2020).
26. Pang, Y.-D., Lee, J. W., Kubota, K. & Ito, H. Solid-state radical C–H trifluoromethylation reactions using ball milling and piezoelectric materials. *Angew. Chem. Int. Ed.* **59**, 22570–22576 (2020).
27. Amer, M. M., Hommelsheim, R., Schumacher, C., Konga, D. & Bolm, C. Electro-mechanochemical approach towards the chloro sulfoximidations of allenes under solvent-free conditions in a ball mill. *Faraday Discuss.* **241**, 79–90 (2023).
28. Wang, Y.-M. et al. Mechanochemical synthesis of 1,2-diketoindolizine derivatives from indolizines and epoxides using piezoelectric materials. *Org. Lett.* **23**, 7171–7176 (2021).
29. Lv, H. G. et al. Mechanochemical divergent syntheses of oxindoles and α-arylacylamides *via* controllable construction of C–C and C–N bonds by copper and piezoelectric materials. *Angew. Chem. Int. Ed.* **61**, e202206420 (2022).
30. Seo, T., Kubota, K. & Ito, H. Dual nickel(II)/mechanoredox catalysis: mechanical-force-driven aryl-amination reactions using ball milling and piezoelectric materials. *Angew. Chem. Int. Ed.* **62**, e202311531 (2023).
31. Wang, G.-F. et al. Solid-state molecular oxygen activation using ball milling and a piezoelectric material for aerobic oxidation of thiols. *RSC Adv.* **12**, 18407–18411 (2022).
32. Wang, X.-H. et al. Mechanochemical synthesis of aryl fluorides by using ball milling and a piezoelectric material as the redox catalyst. *Angew. Chem. Int. Ed.* **62**, e202307054 (2023).
33. He, Y. et al. Piezocatalyzed decarboxylative acylation of quinoxalin-2(1H)-ones using ball milling. *ACS Sustain. Chem. Eng.* **11**, 910–920 (2023).
34. Nothling, M. D., Daniels, J. E., Vo, Y., Johan, I. & Stenzel, M. H. Mechanically activated solid-state radical polymerization and cross-linking *via* piezocatalysis. *Angew. Chem. Int. Ed.* **62**, e202218955 (2023).
35. Wang, X. H. et al. Triphasic hydroxysilylation of alkenes by mechanically piezoelectric catalysis. *Angew. Chem. Int. Ed.* e202410334 (2024).
36. You, F. Z. et al. Mechanochemical vicinal dibromination of unactivated alkenes and alkynes using piezoelectric material as redox catalyst. *Org. Lett.* **26**, 4240–4245 (2024).
37. Qu, R.-L. et al. Mechanical-force-induced non-spontaneous dehalogenative deuteration of aromatic iodides enabled by using piezoelectric materials as a redox catalyst. *Angew. Chem. Int. Ed.* **28**, e202400645 (2024).
38. Xin, X. H. et al. Mechano-photoexcitation for organic synthesis using mechanoluminescent materials as photon sources. *Nat. Synth.* **4**, 177–187 (2025).
39. Patra, S., Nandasana, B. N., Valsamidou, V. & Katayev, D. Mechanochemistry drives alkene difunctionalization *via* radical ligand transfer and electron catalysis. *Adv. Sci.* **11**, 2402970 (2024).
40. Liu, H. D. et al. Redox reactions of organic molecules using a rotating magnetic field and metal rods. *J. Am. Chem. Soc.* **146**, 18143–18150 (2024).
41. Ding, C. Q. et al. Piezoelectrically mediated reversible addition-fragmentation chain-transfer polymerization. *Macromolecules* **55**, 4056–4063 (2022).
42. Wang, Z. H. et al. Enhancing mechanically induced ATRP by promoting interfacial electron transfer from piezoelectric nanoparticles to Cu catalysts. *Macromolecules* **50**, 7940–7948 (2017).
43. Zheng, H. J. et al. Recent advancements in the use of novel piezoelectric materials for piezocatalytic and piezo-photocatalytic applications. *Appl. Catal. B* **341**, 123335–123363 (2024).
44. Liu, W. B., Yang, X. B., Gao, Y. & Li, C. J. Simple and efficient generation of aryl radicals from aryl triflates: synthesis of aryl boronates and aryl iodides at room temperature. *J. Am. Chem. Soc.* **139**, 8621–8627 (2017).
45. Galli, C. Radical reactions of arenediazonium ions: an easy entry into the chemistry of the aryl radical. *Chem. Rev.* **88**, 765–792 (1988).
46. Ghosh, I., Marzo, L., Das, A., Shaikh, R. & König, B. Visible light mediated photoredox catalytic arylation reactions. *Acc. Chem. Res.* **49**, 1566–1577 (2016).
47. Hartmann, M., Li, Y., Mück-Lichtenfeld, C. & Studer, A. Generation of aryl radicals through reduction of hypervalent iodine (III) compounds with TEMPONa: radical alkene oxyarylation. *Chem. Eur. J.* **22**, 3485–3490 (2016).
48. Wang, D., Szillat, F., Fouassier, J. P. & Lalevée, J. Remarkable versatility of silane/iodonium salt as redox free radical, cationic, and photopolymerization initiators. *Macromolecules* **52**, 5638–5645 (2019).
49. Péter, Á., Perry, G. J. P. & Procter, D. J. Radical C–C bond formation using sulfonium salts and light. *Adv. Synth. Catal.* **362**, 2135–2142 (2020).
50. Hu, X.-Q., Liu, Z.-K., Hou, Y.-X. & Gao, Y. Single electron activation of aryl carboxylic acids. *iScience* **23**, 101266–101291 (2020).
51. Schotten, C. et al. Comparison of the thermal stabilities of diazonium salts and their corresponding triazenes. *Org. Process Res. Dev.* **24**, 2336–2341 (2020).
52. Matsuki, Y. et al. Aryl radical-mediated *N*-heterocyclic carbene catalysis. *Nat. Commun.* **12**, 3848–3855 (2021).
53. Zhang, L., Israel, E. M., Yan, J. Y. & Ritter, T. Copper-mediated etherification *via* aryl radicals generated from triplet states. *Nat. Synth.* **1**, 376–381 (2022).
54. Creutz, S. E., Lotito, K. J., Fu, G. C. & Peters, J. C. Photoinduced Ullmann C–N coupling: demonstrating the viability of a radical pathway. *Science* **338**, 647–651 (2012).

55. Le, C., Chen, T. Q., Liang, T., Zhang, P. & MacMillan, D. W. C. A radical approach to the copper oxidative addition problem: trifluoromethylation of bromoarenes. *Science* **360**, 1010–1014 (2018).
56. Ghosh, I., Ghosh, T., Bardagi, J. I. & König, B. Reduction of aryl halides by consecutive visible light-induced electron transfer processes. *Science* **346**, 725–728 (2014).
57. Constantin, T., Juliá, F., Sheikh, N. S. & Leonori, D. A case of chain propagation: α-aminoalkyl radicals as initiators for aryl radical chemistry. *Chem. Sci.* **11**, 12822–12828 (2020).
58. Silva, W. R. C. N., Hellmann, J. E. & Mack, J. Radical reduction of alkyl and aryl halides under mechanochemical conditions. *ACS Sustain. Chem. Eng.* **11**, 14895–14900 (2023).
59. Li, Z. H. et al. Mechanochemical reduction of alkyl and aryl halides using mesoporous zinc oxide. *Chem. Commun.* **60**, 6146–6149 (2024).
60. Hoshina, T., Hatta, S., Takeda, H. & Tsurumi, T. Grain size effect on piezoelectric properties of $BaTiO_3$ ceramics. *Jpn. J. Appl. Phys.* **57**, 0902BB1–0902BB5 (2018).
61. Liu, Y. X. et al. Grain size effect on piezoelectric performance in perovskite-based piezoceramics. *Acta Phys. Sin.* **69**, 217704–217723 (2020).
62. Zheng, P., Zhang, J. L., Tan, Y. Q. & Wang, C. L. Grain-size effects on dielectric and piezoelectric properties of poled $BaTiO_3$ ceramics. *Acta Mater.* **60**, 5022–5030 (2012).
63. Chen, J. W. et al. Shape-tunable $BaTiO_3$ crystals presenting facet-dependent optical and piezoelectric properties. *Small* **19**, 2205920–2205928 (2023).
64. Pramanik, R. et al. Effect of grain size on piezoelectric, ferroelectric and dielectric properties of PMN-PT ceramics. *Ceram. Int.* **45**, 5731–5742 (2019).
65. Smera, S., Biju, K. P. & Binith, M. P. Unveiling the role of defects in optimizing photocatalytic $CaTiO_3$ nanoparticles. *Surf. Interf.* **58**, 105853–105862 (2025).
66. Passi, M. & Pal, B. A review on $CaTiO_3$ photocatalyst: activity enhancement methods and photocatalytic applications. *Powder Technol.* **388**, 274–304 (2021).

Acknowledgements

This work is supported by the National Natural Science Foundation of China (22301192). Sichuan Science and Technology Program (2024NSFSC1124). West China Hospital 135 project (ZYYC23017). Postdoctoral Research Fund of West China Hospital (2024HXBH027). The authors also thank Fenglan Xu and Hui Wang from the Analytical & Testing Center at SichuanUniversity for sample analysis.

Author contributions

Z.L. and X.W. conceived the idea and led the project. X.W. and Q.H. performed the experiments and collected the data. X.W., Q.W., and R.Q. prepared the Supplementary Information. Writing – original draft: X.W. Writing – review & editing: X.W., X.H., Z.L., and X.Z. All authors participated in result discussions and provided feedback on the manuscript.

Competing interests

The authors declare no competing interests.

Additional information

Supplementary information The online version contains supplementary material available at https://doi.org/10.1038/s41467-025-60459-0.

Correspondence and requests for materials should be addressed to Zhong Lian.

Peer review information *Nature Communications* thanks Hui Liu, and Zhao Wang for their contribution to the peer review of this work. A peer review file is available.